ALGORITHMS FOR DETERMINATION OF THE VECTOR VELOCITY FIELD IN A TWO-PHASE GAS-LIQUID FLOW

by

Grzegorz LIGUS[a], Maciej MASIUKIEWICZ[b], Stanislaw ANWEILER[a*], and Marek WASILEWSKI[b]

[a]Faculty of Mechanical Engineering, Opole University of Technology, Opole, Poland
[b]Faculty of Production Engineering and Logistics, Opole University of Technology, Opole, Poland

Original scientific paper
https://doi.org/10.2298/TSCI200323277L

Energy efficiency is a key issue of sustainable development. During the design of industrial devices, it strives to achieve the highest possible energy efficiency. In the industrial systems, two-phase flow is a difficult task, especially the prediction, and maintenance of the two-phase flow regime. That is why this research proposes the evaluation and choice of an algorithm that will give a hint of the device design for which the hydrodynamic conditions of the two-phase mixture flow may be evaluated. The tests were carried out in a rectangular vertical narrow channel, as this type of device is in common use. The work aimed to show which algorithm is better for such evaluation. Parameters such as pressure drop, heat, mass, and momentum transfer are influenced by the phase velocity field. Still, various models are used for the determination of the velocity field. Therefore, there is a problem of choosing a model that will give the results closest to the real conditions. Flow visualization gives the non-invasive determination of the actual velocity field. An analysis of the velocity field was performed, which showed that for different two-phase flow regimes there are differences for given algorithms. The following algorithms were used to determine the velocity vector field: adaptive correlation method and adaptive particle image velocity method were used which are the parts of the general digital particle image velocimetry. The determination of the velocity fields in the quantitative and qualitative assessment of a given two-phase flow regime was obtained. The result of the research is the evaluation of algorithms for characterization two-phase gas-liquid flow.

Keywords: *multiphase systems, flow pattern, image analysis, particle image velocimetry*

Introduction

The flow of two-phase liquids is widespread in the industry. It can be found in such processes as boiling of fluids [1], condensation of vapours [2], transport of fluids [3], heat, mass, and momentum transfer [4], cooling [5], and fluidization [6]. A difficult problem in a precise analysis of the flow of two-phase liquids is the determination of the volumetric share of phases. The volumetric share determines many parameters that are important from the practical point of view. These include pressure drop [7], the efficiency of equipment and pro-

*Corresponding author, e-mail: s.anweiler@po.edu.pl

cesses [8], and thermal-flow coefficients [9]. The material strength parameters, vibration propagation, and reliability of the devices are also dependent on the volumetric share [10]. The phase flow velocity in the process is closely correlated with the parameters previously listed [11]. Therefore, the knowledge of phase flow velocity is necessary to determine these parameters for the intensive development of various measurement techniques and research in this field [12, 13]. One of the most frequently used research techniques is particle image velocimetry (PIV) [14].

The PIV is currently one of the best tools to determine the vector velocity field. In the industrial practice, the application possibilities of this technique have been widely documented, for example in mechanical engineering [15], process engineering [16], medicine [17], environmental engineering [18], and power industry [19]. The most important problem nowadays is the choice of appropriate measurement set-up and its optical and software configuration [14]. Another difficulty is the selection of an appropriate algorithm to determine the velocity field for a given two-flow regime.

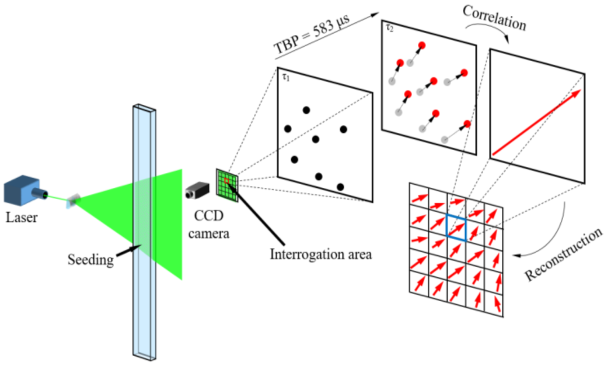

Figure 1. The idea of a method and algorithms

In this paper, we deal with this problem by evaluating the flow using two different algorithms of the DANTEC Dynamic Studio environment [20]. These are the adaptive correlation (AC) algorithm, for which an optimal set of steps has been proposed to achieve high-quality measurement and the adaptive PIV (APIV) algorithm with automatic iterative auto-configuration. fig. 1 and tab. 1 show the idea of a measurement method and algorithms.

Table 1. Comparison of AC and APIV algorithms

Algorithm / Parameter	AC	APIV
Time between pulses	Dependent on the theoretical flow velocity of the liquid phase	Dependent on the theoretical flow velocity of the liquid phase
Size of the interrogation area (IA)	Dimension selection, *e. g.* 16 ×16 pixels Checking the number of visible markers in the IA Control of the tags shift in the consecutive frames If the assumptions are not met, select another dimension [14] In case of compliance with the assumptions of the method, perform a second verification at several other points of the calculation area In the case of positive results, the IA can be considered to be correctly selected	Define the pitch gradient of the assumed IA (grid step size) Define the maximum and minimum size of the IA Specify the particle density in the IA (minimum number of tags and the expected number of tags) Determine the sensitivity of the IA size to a velocity gradient Specify the number of iterations and the convergence limit

Methods and measurement set-up

In the presented research, the evaluation of PIV algorithms, enabling the reconstruction of vector velocity fields, was based on the studies of two-phase gas-liquid flow in a rectangular narrow channel. The requirements of the method impose the necessity to carry out tests with the use of transparent models of devices. For this reason, the model of the tested element was made of polymethyl methacrylate (PMMA). The measuring system is shown in fig. 2, and the details of the flow channel are shown in fig. 3. The flow channel consists of the main channel, the gas phase distribution system, and the liquid phase supply system. The main channel of rectangular cross-section with dimensions 0.05 × 0.0045 m and a length of 1.605 m is placed vertically. In the lower part of the main channel, there was an inlet stub of the liquid phase with a gas distributor in the form of a 0.005 m diameter nozzle where the two-phase mixture was produced. The main channel was terminated with an outlet stub perpendicular to the main direction of liquid flow. Measurement of gas-phase parameters was performed with the use of Alicat Scientific MCR-500SLPM mass-flow meter. The liquid phase circulating in a closed system, after the measurement of the stream using the Enko MPP600 flow meter, is returned to the tank which also acted as a phase separator. The liquid phase was water mixed with a fluorescent seeding particle with a diameter of 1-20 μm (PMMA-RhB-FRAK-SC57-01) using the Rodamine B dye [21]. Compressed air was the gas phase.

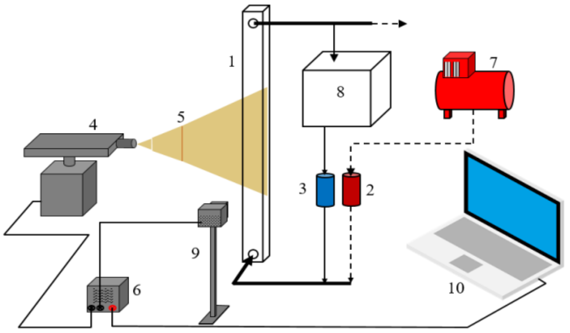

Figure 2. Diagram of the measuring system: *1 – flow channel, 2 – gas-phase flow meter, 3 – liquid phase flow meter, 4 – Nd: YAG laser, 5 – laser sheet, 6 – pulse generator, 7 – compressor, 8 – storage tank with separator, 9 – camera CCD, 10 – control computer for image recording and data processing*

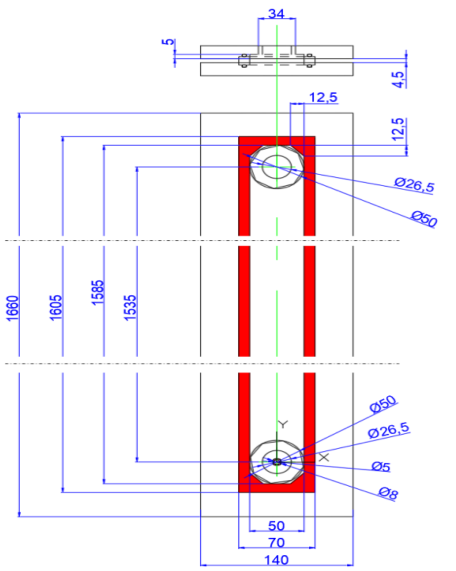

Figure 3. Flow channel details and dimensions

The DPIV measurement system consisted of a laser as a light source, a CCD camera recording the flow phenomena in the measurement channel, and a pulse generator synchronizing both these devices. The entire system was controlled by the Dantec Dynamic Studio 2015a environment. Also in this environment, recording, processing, and image analysis were performed. The two-phase flow regime occurring during the operation of the gas-liquid system required the use of filters acting selectively on the light reaching the camera sensor. To avoid laser light flashes on the extended and dynamic interphase surface, the Omega Optical 550LP filter was used [22], which cuts off 98% of light emission of wavelength lower than 550 nm. Thanks to this, the laser light of 532 nm wavelength did not reach the camera matrix, but only the light excited by it, emitted by fluorescent seeding particles, because it was characterized by wavelength from 610 to 650 nm, *i. e.* above the cut-off threshold. In tab. 2 the used measuring equipment was compared and parameterized.

The measurement method was based on a comparative study of flow parameters securing the occurrence of four two-phase structures during such flow regimes as bubbling, **B**, plug, **P**, slug, **S,** and dispersed slug, **DS,** for the discussed channel. Flow structures were defined based on flow maps, such as in [23]. Table 3 presents the list of two-phase flow structures, flow parameters with corresponding time between pulses (TBP), and corresponding figure to be able to refer to flow maps of different authors [24, 25]. In the flow structure definitions of the referenced flow maps, the authors take a different approach to nomenclature on their research of the two-phase flow regimes. In this work, the nomenclature has been expanded.

Table 2. List of measuring instruments and descriptions of selected configuration parameters.

Parameter	Description
CCD camera	Dantec Dynamics FlowSense EO 4M
Laser	Dantec Dynamics DualPower TR
A pulse generator (synchronizer)	Berkeley Nucleonics Corp Model 575-8
The TBP [μs]	From 292 to 4666 depending on phase flow parameters
PIV algorithms	AC, Adaptive PIV (APIV)
Size of calculation areas (vertical × horizontal) [pixels]	For AC: 32 × 32 (with 50% overlap in both directions) For APIV: variable, dependent on the result of adaptive iteration
Correction of erroneous vectors	Standardized median validation Universal Outlier Detection
Gas-phase flow meter	Alicat Scientific MCR-500SLPM Mass-flow
Liquid phase flow meter	Enko MPP600

Table 3. List of two-phase flow structures, flow parameters with corresponding TBP and Figure.

Flow structure	The volume of liquid, [m^{3}h^{-1}]	Superficial liquid velocity [ms^{-1}]	Volume of gas, [m^{3}h^{-1}]	Superficial gas velocity [ms^{-1}]	TBP [μs]	Corresponding figure
Bubbling – B	0.4	0.44	0.025	0.0275	583	fig. 5
Plug – P	0.4	0.44	0.05	0.0550	583	fig. 6
Slug – S	0.4	0.44	0.2	0.2200	583	fig. 7
Dispersed **S**lug – DS	0.4	0.44	0.6	0.6601	583	fig. 8

For the presentation of the results, 4 examples from 30 series of measurements were selected. Each consisted of 100 consecutive images of two-phase flow structures recorded by the camera operating in double frame mode. The raw images were pre-processed to determine the measurement area, to compensate for the histogram of images brightness using a defined pixel brightness balance, and to isolate moving seeding particles from the images by arithmetic (see fig. 4). The prepared material was used as a basis for the reconstruction of the vector velocity field using two algorithms AC and APIV. The average vector field obtained from each series was subjected to the operation of removing the wrong vectors using standardized median validation. The obtained vector velocity fields in both cases were converted to a scalar velocity field and the velocity histogram was determined to identify local differences. The capture of global characteristics required the use of the power spectral density (PSD) function. Based on the divergence of the PSD function, the phase velocity values extracted from the series of 100 images in the selected measurement area were used. The detailed procedure is shown schematically in fig. 4.

Results and discussion

The use of the imaging and image analysis techniques described above allowed to compare the performance of the two algorithms to determine the vector velocity field using the

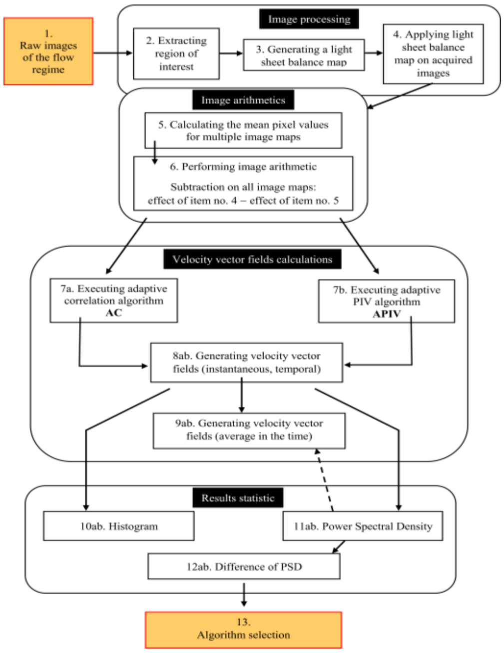

Figure 4. Block diagram of the test method

PIV method for two-phase fluid-flow. Due to the dynamic nature of the two-phase fluid-flow, the vast majority of analyses concern averaged dynamic parameters such as phase flow velocity, void fraction, the density of the mixture, pressure drops, gas holdup rate, *etc*. Therefore, in the presented studies, the selection of algorithms for the determination of velocity fields was focused mainly on statistical evaluation. As a result of the conducted research and measurements, data and calculations were collected and presented in graphic form on the following drawings (figs. 6-9). The following convention was adopted in the drawings: visualization of a selected structure of two-phase fluid-flow is presented, reconstruction of a momentary velocity field with the use of both studied algorithms (AC, APIV) at a given moment corresponding to the structure in the image is presented, subsequent reconstructions concern the averaged velocity field for the duration of the whole series of measurements. Additionally, statistical characteristics (histogram, Power Spectrum Density) corresponding to a given structure are presented.

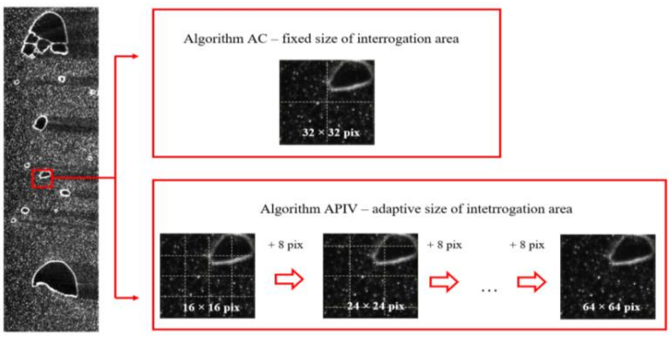

Figure 5. The IA sizing in both algorithms

Figure 5 shows a comparison of the IA for both evaluated algorithms and how to change the size of the IA on the selected example of the two-phase flow pattern. It shows the way of grid development in subsequent iterations of IA adaptation for the given APIV case. Based on the analysis of the results shown in figs. 6-9, histogram differences were observed for both algorithms within the same structure, which was also confirmed by the comparison of their mean values. Moreover, a comparative analysis of PSD within the same structure showed differences that increased as turbulence increased. Therefore, it was decided to compare the PSD differences between the structures, as shown in fig. 10.

If the discrepancy is close to zero (as for B, P, S structures), then for this flow regime the algorithm selection has less influence on the results. If the values start to significantly

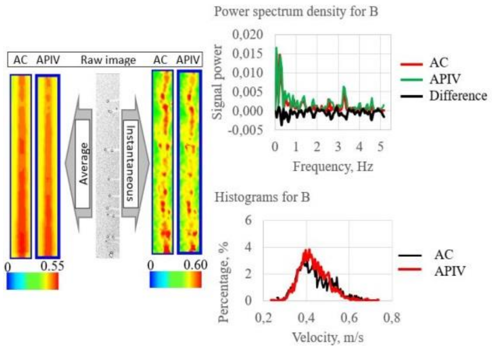

Figure 6. Reconstruction of the vector velocity field and statistical characteristics for the bubble flow structure (for details see tab. 3)

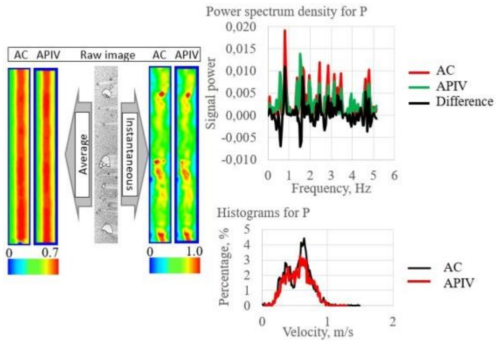

Figure 7. Reconstruction of the vector velocity field and statistical characteristics for the plug flow structure (for details see tab. 3)

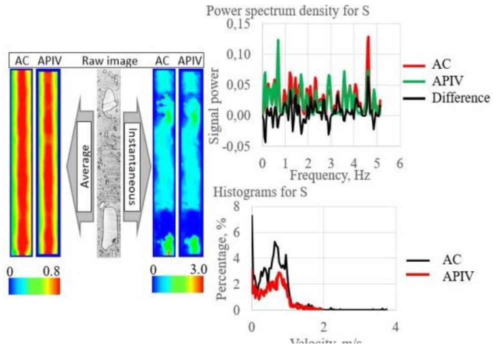

Figure 8. Reconstruction of the vector velocity field and statistical characteristics for the slug flow structure (for details see tab. 3)

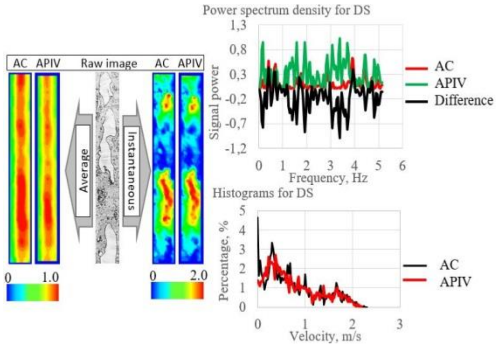

Figure 9. Reconstruction of the vector velocity field and statistical characteristics for the dispersed slug flow structure

different from zero (as in the case of the DS structure), the choice of the algorithm type is important. Theoretically, both algorithms (AC, APIV) offer the possibility to achieve convergent results. However, it is important that for the AC algorithm, the selection of the IA may be associated with multiple manual iterations of parameter configuration. In the APIV algorithm, the parameter selection is adaptive - the algorithm performs a specified number of iterations and selects from among them the size of the IA most suitable for the assumptions of the PIV method (see fig. 5). As a consequence of changing the size of the IA, the control of the number and shift of tags is done without operator intervention. In AC, changes to all these parameters must be changed manually while tracking changes in position and number of seeding particles. The APIV algorithm is therefore characterized by a high level of automation, which is crucial, especially for less experienced operators. Therefore, the APIV generally generates a better reconstruction of the vector velocity field. The slug S structure has the greatest number of small bubbles, whose interphase surface is highly reflective, so with a constant IA (as for AC), it can be wrongly identified as a set of marker particles, which overstates the identified velocities and enlarges the histogram. This is one of the reasons why for this case APIV is better than AC. APIV has one disadvantage – it extends the research process because of the iterative repetition of calculations necessary to correctly find the dimensions of the IA.

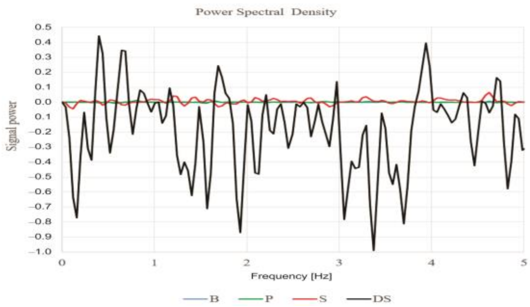

Figure 10. Comparison of PSD function discrepancies for AC and APIV algorithms for each flow structure tested

When it is necessary to quickly reconstruct the vector flow field for systems with known geometry and known flow parameters, *e. g.* repetitive, typical flows whose hydrodynamic characteristics are already identified, the AC algorithm seems to be more suitable for use. Thanks to it, with high probability, it allows the proper size of IA choice for such flow cases. The APIV algorithm will look for the right solution from the beginning, testing a significant number of incorrect combinations.

Conclusions

Differences in phase velocity values in the histograms for the AC and APIV algorithms indicate that the process of selecting the size of the IA has a significant influence on the final results. This is because the size of the IA in the AC algorithm is fixed while the size of the IA in the APIV algorithm is variable and adapts. We believe that for the industrial two-phase flow equipment design calculations, the AC calculation algorithm can be successfully used. AC algorithm, even though it is simpler and easier to perform, gives similar results and the calculation time is significantly reduced. However, to use the AC algorithm, the phases of the two-phase mixture have to move in orderly condition, *i. e*. during homogeneous phase distribution. In the case of the high variability of flow in time, as in the case of more turbulent structures, the AC algorithm generates serious discrepancies (see fig. 9). This work has proven that in some cases it is possible to shorten the calculation time and use AC because the result will not differ from the APIV. And reduced calculation time enables faster response in case of automated process control.

In industry and design, simplifications and generalizations are often introduced to make calculations faster. The main goal of the article has been achieved - it has been shown that for some of the flow types it is possible to replace the time-consuming APIV method and calculate vectors using AC because it gives results similar to those of APIV. At this stage of research, each case still has to be considered individually regardless of the flow rate because other factors also influence the two-phase flow regime (*e. g.* flow geometry or pressure). By extending the method proposed in this article for selecting an appropriate PIV algorithm with knowledge of a wider range of two-phase flow hydrodynamics it will be possible to automate the decision-making process.

Based on the literature review and the performed research, the current state of knowledge was enhanced by the analysis of the principles for the selection of PIV method algorithms for the evaluation of two-phase gas-liquid flow patterns and structures in narrow rectangular channels.

Nomenclature

AC – adaptive correlation
APIV – adaptive PIV
DPIV – digital PIV
IA – interrogation area
PIV – particle image velocimetry
PSD – power spectral density
TBP – time between pulses [μs]

References

[1] Mantelli, M. B,. Thermosyphon Technology for Industrial Applications, in: *Heat Pipes and Solid Sorption Transformations: Fundamentals and Practical Applications* (Eds. L.L Vasiliev, S. Kakac), CRC Press, Taylor & Francis Inc., Boca Renton, Fla., USA, 2013, pp. 411-46

[2] Pabon, N. Y. L., *et al.*, Visualization and Experimental Analysis of Geyser Boiling Phenomena in Two-Phase Thermosyphons, *Int. J. Heat Mass Transf.*, *141* (2019), Oct., pp. 876-890

[3] Ligus, G., *et al.*, A New Method of Selecting the Airlift Pump Optimum Efficiency at Low Submergence Ratios with the Use of Image Analysis, *Energies*, *12* (2019), 4, pp. 1-19

[4] Wasilewski, M., Brar, L. S., Optimization of the Geometry of Cyclone Separators Used in Clinker Burning Process: A Case Study, *Powder Technol.*, *313* (2017), May, pp. 293-302

[5] Bohdal, T., *et al.*, High Pressure Refrigerants Condensation in Vertical Pipe Minichannels, *Int. J. Heat Mass Transf.*, *134* (2019), May, pp. 1250-1260

[6] Anweiler, S., Ulbrich, R., Flow Pattern for Different Fluidization Apparatuses, *Inzynieria Chemiczna i Procesowa*, *25* (2004), 3, pp. 577-582

[7] Mortazavi, M., Tajiri, K., Two-phase Flow Pressure Drop in Flow Channels of Proton Exchange Membrane Fuel Cells: Review of Experimental Approaches, *Renew. Sust. Energ. Rev.*, *45* (2015), May, pp. 296-317

[8] Radwan, A., *et al.*, Thermal Management of Concentrator Photovoltaic Systems Using Two-phase Flow Boiling in Double-layer Microchannel Heat Sinks, *Appl. Energy*, *241* (2019), May, pp. 404-419

[9] Xie, J., *et al.*, A Comprehensive Understanding of Enhanced Condensation Heat Transfer Using Phase Separation Concept, *Energy*, *172* (2019), Apr., pp. 661-674

[10] Sadek, O., *et al.*, Numerical Investigation of the Cross flow Fluidelastic Forces of Two-phase Flow in Tube Bundle, *J Fluids Struct*, *79* (2018), May, pp. 171-186

[11] Hetsroni, G., *Handbook of Multiphase Systems*, McGraw-Hill Inc., New York, USA, 1982

[12] Anweiler, S., Development of Videogrammetry as a Tool for Gas-particle Fluidization Research, *J. Environ. Manage.*, *203* (2017), Mar., pp. 942-949

[13] Anweiler, S., Masiukiewicz, M., Application of Stereology for Two-phase Flow Structure Validation in Fluidized Bed Reactors, *Thermal Science*, *20* (2016), 4, pp. 1199-1208

[14] Adrian, R. J., Westerweel, J., *Particle Image Velocimetry*, Cambridge University Press, New York, USA, 2011

[15] Ke, S., *et al.*, Aerodynamic Performance and Wind-induced Effect of Large-scale Wind Turbine System Under Yaw and Wind-rain Combination Action, *Renew. Energy*, *136* (2019), June, pp 235-253

[16] Ludwig, W., *et al.*, Analysis of Pneumatic Nozzle Operation With the Stochastic Euler-Lagrange Model, *Chem. Eng. Sci.*, *197* (2019), Apr., pp. 386-403

[17] Yazdi, S.G., *et al.*, A Novel Fabrication Method for Compliant Silicone Phantoms of Arterial Geometry for Use in Particle Image Velocimetry of Haemodynamics, *Appl. Sci.*, *9* (2019), 18, pp. 1-12

[18] Wasilewski, M., *et al.*, Experimental and Numerical Investigation on the Performance of Square Cyclones With Different Vortex Finder Configurations, *Sep. Purif. Technol.*, *239* (2020), May, pp. 116-588

[19] Hutli, E., *et al.*, Experimental and Numerical Investigation of Coolant Mixing in a Model of Reactor Pressure Vessel Down-comer and in Cold Leg Inlets, *Thermal Science*, *21* (2017), 3, pp. 1491-1502

[20] ∗∗∗, www.dantecdynamics.com/particle-image-velocimetry

[21] ∗∗∗, www.dantecdynamics.com/fpp-fluorescent-polymer-particles

[22] ∗∗∗, www.omegafilters.com/product-types/standard-longpass-shortpass

[23] Wilmarth, T., Ishii, M., Two-phase Flow Regimes in Narrow Rectangular Vertical and Horizontal Channels, *Int. J. Heat Mass Transf.*, *37* (1994), 12, pp. 1749-1758

[24] Taitel, Y., *et al.*, Modelling Flow Pattern Transitions for Steady Upward Gas-liquid Flow in Vertical Tubes, *AIChE J*, *26* (1980), 3, pp. 345-354

[25] Kaichiro, M., Ishii, M., Flow Regime Transition Criteria for Upward Two-phase Flow in Vertical Tubes, *Int. J. Heat Mass Transf.*, *27* (1984), 5, pp. 723-737

Paper submitted: March 23, 2020
Paper revised: April 20, 2020
Paper accepted: June 6, 2020